CERN-INTC-2023-023 / INTC-P-661
11/01/2023

EUROPEAN ORGANIZATION FOR NUCLEAR RESEARCH

Proposal to the ISOLDE and Neutron Time-of-Flight Committee

Probing structural transitions in M(II) vanadates (M = Zn, Mn, Cd, Ca) with TDPAC spectroscopy

January 11, 2023

A. Burimova[1], A. W. Carbonari[1], J. H.- Schell[2,3], O. F. S. Leite Neto[1], R. N. Saxena[1], T. N. S. Sales[1], F. A. Genezini[1], L. F. D. Pereira[1], I. S. Ribeiro Junior[1], B. S. Correa[1], N. P. de Lima[1], A. A. Miranda Filho[1], G. A. Cabrera-Pasca[4], D. Richard[5], J. G. M. Correia[2,6], D. C. Lupascu[3], A. M. Gerami[2,7]

[1]*Instituto de Pesquisas Energéticas e Nucleares. IPEN, São Paulo, SP, Brazil*
[2]*European Organization for Nuclear Research (CERN), CH-1211 Geneva, Switzerland*
[3]*Institute for Materials Science and Center for Nanointegration Duisburg-Essen (CENIDE), University of Duisburg-Essen, 45141 Essen, Germany*
[4]*Universidade Federal do Pará, Campus de Abaetetuba, Pará, Brazil*
[5]*Departamento de Física, Facultad de Ciencias Exactas, Universidad Nacional de La Plata, La Plata, Argentina*
[6]*Centro de Ciências e Tecnologias Nucleares (CCTN), IST, Universidade de Lisboa, Portugal*
[7]*School of Particles and Accelerators, Institute for Research in Fundamental Sciences (IPM), Tehran P.O. Box 19395-5531, Iran*

Spokesperson: Anastasia Burimova anstburimova@gmail.com, Artur Wilson Carbonari carbonar@ipen.br, Juliana H.-Schell juliana.schell@cern.ch
Technical coordinator: Juliana H.-Schell juliana.schell@cern.ch

Abstract:

We propose an investigation of structural phase transitions in bivalent metal (M = Zn, Mn, Cd, Ca) meta- and pyrovanadates at a local scale with nuclear methods. We intend to establish the conditions for M vanadate cluster formation in V_2O_5:M solid solutions, among which the lower limit for M concentration. The refined information on vanadate nucleation and transition paths is expected to be practical for novel research on charge (de)intercalation mechanisms in metal-ion aqueous batteries with vanadia-based electrodes.

Requested protons: 8 shifts protons on target, (split into 4 runs over 2 year)
Experimental Area: GLM area, ISOLDE hall or offline laboratories

1 Introduction and motivation

In recent years the research on rechargeable metal-ion (M) aqueous batteries (MAB) continued gaining popularity due to their safety and economic benefits on one hand and the necessity for improving their performance on the other.
The reaction mechanism allowing energy storage in MAB remains obscure, though the general assumption is that the insertion (extraction) of M and/or H^+ ions to (from) the cathode structure occurs upon charge (discharge) steps (see [1] and references therein). Evidently, the charge transport and storage efficiency are significantly affected by the architecture of the host. The use of layered materials for charge hosting, among which hydrous V_xO_y-based compounds, allowed an enhanced MAB performance, and in later works, the inter-layer spacing of these cathode candidates was artificially extended via pillaring the layers with either pre-intercalated carrier metal ions or other elements [2–8]. It is noteworthy that the synthesis method commonly employed to produce V_xO_y-based cathode substances, the hydrothermal route, does not guarantee structural integrity and uniformity. The introduction of guest atoms for pillaring, as well as irreversible trapping of carrier M ions upon cycling, may also result in structural collapse of V_xO_y, e.g. provoke the formation of contaminant stoichiometric vanadate clusters, especially upon specific operation conditions. In this regard, it is important to define the critical concentrations of M in V_xO_y:M from which the nucleation of M vanadates becomes possible, since even a small admixture of the contaminant may affect the performance of the electrode.
The role of stoichiometric vanadates in V_xO_y-based MAB is essential at the stage of waste management as well. Large-scale spent batteries give rise to massive waste and thus to a strong demand for effective recycling strategies. For vanadia-based Li-ion batteries an easy and green approach was proposed by Du *et al.* lately in 2019 [9]. Short annealing at 773K of Li^+ charged V_2O_5 in a muffle furnace has led to the formation of LiV_3O_8 which, in its turn, demonstrated an appropriate performance as Li host.
Notably, at a fully charged state of hydrous V_2O_5-based cells, the nominal atom number ratio of Zn (acting as both carrier and pillar) and V was 1.35:2, which is greater than in Zn meta- (ZnV_2O_6) and smaller than in pyrovanadate ($Zn_2V_2O_7$) [2]. Therefore, one would expect the presence of these phases upon recycling-targeted thermal procedures similar to those of Du *et al.* above described. To the excitement of the environmentally conscious community, α-$Zn_2V_2O_7$ performance as MAB (M = Zn) cathode material was already tested and found acceptable [4, 10]. Therefore, there is an evident potential in developing the routes of adoption of the (mixed) vanadate products as the new cathode candidates, as a way for V_xO_y-based MAB to meet the norms of contemporary environmental ethics.

Meta- and pyrovanadates of bivalent metals may exhibit polymorphism and their properties are structure-dependent. E.g. MnV_2O_6 suffers a transition from brannerite (B) to pseudobrannerite (P) near 700 – 800K and so does CdV_2O_6 at lower temperature as illustrated in Fig. 1 [11]. The metastable P phase, offering wider channels for ion transfer, may stabilize at lower temperatures. Notably, the reverse P→B transition upon cooling was reported to have explosive character and to occur at temperatures as low as $\sim$ 350K [11]. Hence, according to earlier findings, depending on concentration and operation conditions, metavanadate P phase may either be beneficial for MAB applications or compromise their functioning. This example emphasizes the importance of detailed

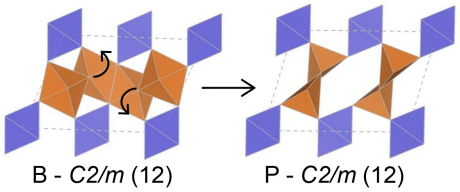

Figure 1: An illustration of B to P structure transition in MnV_2O_6

unambiguous information on structural transitions in cathode-suitable vanadates. To expand the currently available scope of structure data we propose a detailed study of local structural peculiarities in meta- and pyrovanadates of Zn, Mn, Cd, and Ca with hyperfine-interactions(HFI)-based time differential perturbed angular correlation spectroscopy (TDPAC).

2 Objectives

The implementation of current proposal involves

i Mapping the hyperfine parameters ($|V_{zz}|$, η, B_{hf}) for bivalent M meta- and pyrovanadates (M = Zn, Mn, Cd, Ca) in a wide range of temperatures and, consequently, interpreting them unambiguously. To our knowledge, such data is currently unavailable except for a study of hyperfine interactions at the V site with ^{51}V nuclear magnetic resonance spectroscopy [12];

ii Rectification of the paths of structural transitions in the compounds above specified, including magnetic transitions in Mn vanadates [13, 14];

iii Determination of critical concentrations of M in $M_xV_{2-x}O_5$ at which a structural collapses to stoichiometric M(II) vanadates occur. Determination of structural collapse scenario (if any) to meta- or pyro- vanadates (or their combination) upon temperature;

iv Studying the relation between sample composition/local structure and morphology/synthesis method.

3 Description of the proposed work

3.1 Route to achieve the proposed objectives

The local structure of the samples and its evolution with temperature is intended to be probed with TDPAC spectroscopy taking advantage of ^{111}In and $^{111\mathrm{m}}$Cd parent isotopes at home institution and ISOLDE respectively.
A conventional approach to the analysis of TDPAC data consisting in complementing experimental results with *ab initio* simulations within Density Functional Theory (DFT) is to be adopted for the identification of the observed hyperfine interactions. This strategy has demonstrated efficiency for a large series of binary oxides (see [15] and references

therein) but has its limitations. One of those is the tendency to, adjust the "input" and "settings", and manage the theoretical "output" forcing it to coincide with experimental results somewhat compromising the *ab initio* principle.
Moreover, our previous TDPAC experiments with nominal CdV_2O_6 have revealed 3 distinct interactions, two of which were present within a wide temperature range, 300 – 800K, a fact that hindered their identification and multiplied the number of possible "input" options for calculations (e.g. defective sites of diverse types should be simulated as well) making them costly.
To compensate for this, we opted for a family of vanadates that, beyond responding to practical interests, were demonstrated to have structures convenient for comparative analysis. E.g. as mentioned above, ZnV_2O_6 crystallizes in B and does not suffer a transition to P-phase, CdV_2O_6, and MnV_2O_6 both suffer the B→P transition, but at quite distinct temperatures, and CaV_2O_6 possesses P structure in the whole temperature range. Since structural parameters of all B phases are quite similar (same for P), one expects the M = Zn, Ca data (unchanged phases) to help identify the interactions in metavanadates with transitions.
The melting point of pyro-vanadates is higher than that of meta-vanadates, so the measurements at elevated temperatures (for the mixed-phase samples of smaller volume) are expected to provide structural information on pyro-vanadates alone. Here we note that our group has successfully applied this strategy for $Eu_3Ir_4Sn_{13}$ alloy to eliminate the contribution of metallic Sn, a synthesis-induced contaminant, from TDPAC data via performing measurements at temperatures above 500K (i.e. above Sn melting point).

3.2 Preparation and characterization of samples at home institution

The samples will be obtained following 3 main synthesis routes: hydrothermal procedure (the most popular for the preparation of MAB cathode candidates, resulting in nanoscale morphologies), sol-gel (a simpler method yet implying carbon residue helpful to simulate chemical bonding with C at sample surface), solid-state reaction (a simple method free of contamination with non-native elements allowing sample standards for a comparative study). Since the relation between preparation conditions and phase composition is an important practical issue, the former per se are the parameters in our analysis. The deviations from nominal M concentrations will be tracked with neutron activation analysis at the home institution.
Prior to and after TDPAC experiments the samples will be characterized with X-ray diffraction, electron microscopy (morphology and structure investigation, important as morphology affects cathode performance), and possibly X-ray photoelectron spectroscopy (expected to be soon available at home institution). A partial description of the above supplementary home infrastructure may be found here.
We emphasize that isolating a single allotrope of either vanadia or vanadate is a major challenge, though, for the case of Cd and Zn vanadates, reasonable results were already achieved at the home institution.

3.3 DFT simulations

To be performed independently at the home institution and CERN with the help of the WIEN2k package employing full-potential augmented plane waves plus local orbitals as a basis set.

3.4 The rationale for TDPAC application

3.4.1 Why TDPAC?

In some sense, TDPAC spectroscopy has a simultaneous power of several conventional methods at the local level, *i.e.* it provides information on site geometry (may reveal information on a crystalline structure similar to a conventional diffraction experiment but locally); the dynamic interactions related to the charge density alteration may be associated with collective excitations alternatively probed with Raman spectroscopy; the charge state of the impurity site usually revealed in combination with DFT analysis has some analogy with insights provided by photoelectron spectroscopy. While trace amounts of contaminants may pass unnoticed by conventional techniques, TDPAC may reveal the presence of minor phases [16].
Moreover, this HFI-based method allows measurements at a variety of conditions, including high and low temperatures, pressure, gaseous environment, or dynamic vacuum, and the laboratories at ISOLDE and home institution are fully equipped to reproduce these conditions. This is of particular interest as with the current proposal we aim at rectification of structure transition paths, including the peculiarities of magnetic ordering in Mn vanadate at low temperatures.
Probe ions introduced to the samples to be studied with TDPAC, albeit highly diluted, serve as an imitation of dopants. This contributes to the practical benefits of TDPAC, as doping is one of the strategies for cathode performance enhancement.

3.4.2 Why TDPAC with ^{111m}Cd?

Let us summarize the benefits of ^{111m}Cd parent for the proposed investigation:

i No after-effect, in contrast to ^{111}In (to be used at home institution);

ii May have site affinity different from ^{111}In providing complementary data. E.g. for Mn-vanadates In is expected to occupy the Mn site, whereas Cd may reside at the V site or interstitial position; in Cd and Zn vanadates ^{111m}Cd is expected to substitute M site;

iii Even if ^{111}In and ^{111m}Cd occupy the same type of sites, they may induce different charge states at the impurity leading, again, to complementary data;

iv The ionic radii R of In and Cd in 6-fold coordination satisfy $R(\mathrm{Mn}) < R(\mathrm{Zn}) < R(\mathrm{In}) < R(\mathrm{Cd}) < R(\mathrm{Ca})$, where the set of first 3 and that of the last 2 have closer values [17]. So, employing both ^{111}In and ^{111m}Cd in our study for each compound one

may imitate 3 possibilities: (0) undoped structure of Cd vanadates, (1) minor structural relaxations around the dopant and (2) pronounced distortions due to significant chemical pressure or, alternatively, interstitial doping.

3.5 Report: Resume of earlier findings

The summary of the previous findings including our preliminary experimental and theoretical insights is presented in Table 1. We emphasize that this set reveals a great number of gaps and some contradictions that we intend to complete and resolve.

Table 1: The summary on the hyperfine parameters data available for meta- and pyrovanadates of interest. The references are absent when our findings within the current project are cited. Those include TDPAC and DFT insights.

(attributed) Site	Experimental		Theoretical	
	V_{zz}, 10^{21} V/m^2	η	V_{zz}, 10^{21} V/m^2	η
ZnV_2O_6 (B): [Zn]	-	-	-7.96 [18]	0.46 [18]
ZnV_2O_6 (B): [V]	5.46 [12]	0.4 [12]	4.88 [18]	0.42 [18]
			-5.40 [19]	0.45 [19]
MnV_2O_6 (B): [Mn]	-	-	-6.27 [18]	0.69 [18]
MnV_2O_6 (B): [V]	-	-	4.87 [18]	0.11 [18]
MnV_2O_6 (P): [Mn]	-	-	-	-
MnV_2O_6 (P): [V]	-	-	-	-
CdV_2O_6 (B): [Cd]	6.25	0.38	-5.34 [18]	0.97 [18]
			5.93	0.77
CdV_2O_6 (B): [V]	5.14 [12]	0.47 [12]	4.25 [18]	0.48 [18]
			5.08	0.87
CdV_2O_6 (P): [Cd]	-	-	-	-
CdV_2O_6 (P): [V]	1.35 [12]	1 [12]	-	-
CaV_2O_6 (P): [Ca]	-	-	-	-
CaV_2O_6 (P): [V]	2.43 [12]	0.51 [12]	-	-
$Zn_2V_2O_7$: [Zn]	9.62	0.41	-	-
$Zn_2V_2O_7$: [V]	-	-	-2.71 [19]	0.69 [19]
$Cd_2V_2O_7$: [Cd]	6.52	0.36	-	-
$Cd_2V_2O_7$: [V]	-	-	-4.28 [19]	0.36 [19]

4 Summary of the requested protons

We estimate the total amount of ISOLDE beam time needed to implement the proposal as 8 shifts distributed according to Table 2.

Table 2: Beam time request for TDPAC studies

Required isotope	Implanted beam	Probe element	Type of exp.	Approx. Intensity [at/μC]	Target/Ion source	Required atoms per sample	# of shifts
^{111m}Cd (48m)	^{111}Cd	^{111}Cd	$\gamma-\gamma$ PAC	10^8	Sn target; VD 5 ion source	2×10^{10}	8
Total # of requested shifts							**8**

References

[1] S. Bi, S. Wang, F. Yue, Z. Tie, and Z. Niu. A rechargeable aqueous manganese-ion battery based on intercalation chemistry. *Nature Communications*, 12(6991), 2021. doi: 10.1038/s41467-021-27313-5.

[2] D. Kundu, B. D. Adams, V. Duffort, S. H. Vajargah, and L. F. Nazar. A high-capacity and long-life aqueous rechargeable zinc battery using a metal oxide intercalation cathode. *Nature Energy*, 1(16119):1–8, 2016. doi: 10.1038/NENERGY.2016.119.

[3] J. Ding, Z. Du, L. Gu, B. Li, L. Wang, S. Wang, Y. Gong, and S. Yang. Ultrafast Zn^{2+} intercalation and deintercalation in vanadium dioxide. *Advanced Materials*, 30(26):(1800762) 1–6, 2018. doi: 10.1002/adma.201800762.

[4] C. Liu, Z. Neale, J. Zheng, X. Jia, J. Huang, M. Yan, M. Tian, M. Wang, J. Yang, and G. Cao. Expanded hydrated vanadate for high-performance aqueous zinc-ion batteries. *Energy Environ. Sci.*, 12:2273–2285, 2019. doi: 10.1039/c9ee00956f.

[5] J. Zheng, C. Liu, M. Tian, X. Jia, E. P. Jahrman, G. T. Seidler, S. Zhang, Y. Liu, Y. Zhang, C. Meng, and G. Cao. Fast and reversible zinc ion intercalation in Al-ion modified hydrated vanadate. *Nano Energy*, 70(104519):1–10, 2020. doi: 10.1016/j.nanoen.2020.104519.

[6] W. Zhou, M. Chen, A. Wang, A. Huang, J. Chen, X. Xu, and C.-P. Wong. Optimizing the electrolyte salt of aqueous zinc-ion batteries based on a high-performance calcium vanadate hydrate cathode material. *Journal of Energy Chemistry*, 52:377–384, 2021. doi: 10.1016/j.jechem.2020.05.005.

[7] C. Xia, J. Guo, P. Li, X. Zhang, and H. N. Alshareef. Highly stable aqueous zinc-ion storage using layered calcium vanadium oxide bronze cathode. *Angew. Chem.*, 57(15):3943–3948, 2018. doi: 10.1002/ange.201713291.

[8] Y. Wu, Z. Zhu, Y. Li, D. Shen, L. Chen, T. Kang, X. Lin, Z. Tong, H. Wang, and C. Lee. Aqueous MnV_2O_6-zn battery with high operating voltage and energy density. *Small*, 17 (2008182):1–9, 2011. doi: 10.1002/smll.202008182.

[9] L. Du, H. Lin, Z. Ma, Q. Wang, D. Li, Y. Shen, W. Zhang, K. Rui, J. Zhu, and W. Huang. Using and recycling V_2O_5 as high performance anode materials for sustainable lithium ion battery. *Journal of Power Sources*, 424:158–164, 2019. doi: 10.1016/j.jpowsour.2019.03.103.

[10] H. Liu and Y. Cui. Microwave-assisted hydrothermal synthesis of hollow flower-like $Zn_2V_2O_7$ with enhanced cycling stability as electrode for lithium ion batteries. *Materials Letters*, 228(1):369–371, 2018. doi: 10.1016/j.matlet.2018.06.056.

[11] K. Mocala and J. Ziólkowski. Polymorphism of the bivalent metal vanadates MeV_2O_6 (Me = Mg, Ca, Mn, Co, Ni, Cu, Zn, Cd). *Journal of Solid State Chemistry*, 69(2):299–311, 1987. doi: 10.1016/0022-4596(87)90087-9.

[12] U. G. Nielsen, H. J. Jakobsen, and J. Skibsted. Characterization of divalent metal metavanadates by ^{51}V magic-angle spinning NMR spectroscopy of the central and satellite transitions. *Inorg. Chem.*, 39:2135–2145, 2000. doi: 10.1021/ic991243z.

[13] S. A. J. Kimber and J. P. Attfield. Disrupted antiferromagnetism in the brannerite MnV_2O_6. *Phys Rev B*, 75(064406):1–4, 2007. doi: 10.1103/PhysRevB.75.064406.

[14] Z. He and Y. Ueda. Magnetic properties of $Mn_2V_2O_7$ single crystals. *Journal of Solid State Chemistry*, 181:235–238, 2008. doi: 10.1016/j.jssc.2007.11.028.

[15] A. Burimova, A. W. Carbonari, N. P. de Lima, A. A. M. Filho, A. P. d. S. Souza, T. d. S. N. Sales, W. L. Ferreira, L. F. D. Pereira, B. S. Correa, and R. N. Saxena. Local crystalline structure of doped semiconductor oxides characterized by perturbed angular correlations: Experimental and theoretical insights. *Crystals*, 12(9):1204, 2022. doi: 10.3390/cryst12091204.

[16] C. M. Rivaldo-Gómez, G. A. Cabrera-Pasca, A. Zúñiga, A. W. Carbonari, and J. A. Souza. Hierarchically structured nanowires on and nanosticks in ZnO microtubes. *Sci Rep*, 5: 15128, 2015. doi: 10.1038/srep15128.

[17] P. W. Atkins, T. L. Overton, J. P. Rourke, M. T. Weller, and F. A. Armstrong, editors. *Shriver and Atkins' Inorganic Chemistry, Fifth Edition*, chapter Resource section 1. Oxford University Press, Great Britain, 2010. ISBN 978-1-42-921820-7.

[18] K. Choudhary, J. N. Ansari, I. I. Mazin, and K. L. Sauer. Density functional theory-based electric field gradient database. *Scientific Data*, 7(362), 2020. doi: 10.1038/s41597-020-00707-8.

[19] A. Y. H. Lo, J. V. Hanna, and R. W. Schurko. A theoretical study of ^{51}v electric field gradient tensors in pyrovanadates and metavanadates. *Applied Magnetic Resonance*, 32: 691–708, 2007. doi: 10.1007/s00723-007-0045-9.

Appendix

DESCRIPTION OF THE PROPOSED EXPERIMENT

Part of the experiment	Design and manufacturing
SSP implantation chamber located at the GLM area	☒ To be used without any modification ☐ To be modified
Part 1: Annealing furnaces located at 508/R-004	☒ Standard equipment supplied by a manufacturer ☐ CERN/collaboration responsible for the design and/or manufacturing
Perturbed angular correlation spectrometers existing in the building 508	☒ Standard equipment supplied by a manufacturer ☒ CERN/collaboration responsible for the design and/or manufacturing
[insert lines if needed]	

HAZARDS GENERATED BY THE EXPERIMENT
Additional hazard from flexible or transported equipment to the CERN site:

Domain	Hazards/Hazardous Activities		Description
Mechanical Safety	Pressure	☒	N2 2 bar, 1 l
	Vacuum	☒	10^{-6} mbar at SSP chamber 10 during collections and 10^{-5} mbar at part 1
	Machine tools	☐	
	Mechanical energy (moving parts)	☐	
	Hot/Cold surfaces	☒	RT - 800 K
Cryogenic Safety	Cryogenic fluid	☐	[fluid] [m3]
Electrical Safety	Electrical equipment and installations	☒	Compressor and water system 10 A
	High Voltage equipment	☒	Up to 2 kV for TDPAC detectors
Chemical Safety	CMR (carcinogens, mutagens and toxic to reproduction)	☐	[fluid], [quantity]

	Toxic/Irritant	☐	[fluid], [quantity]
	Corrosive	☐	[fluid], [quantity]
	Oxidizing	☐	[fluid], [quantity]
	Flammable/Potentially explosive atmospheres	☐	[fluid], [quantity]
	Dangerous for the environment	☐	[fluid], [quantity]
Non-ionizing radiation Safety	Laser	☐	[laser], [class]
	UV light	☐	
	Magnetic field	☐	[magnetic field] [T]
Workplace	Excessive noise	☐	
	Working outside normal working hours	☒	Yes, if beam time is scheduled 24 h per day.
	Working at height (climbing platforms, etc.)	☐	
	Outdoor activities	☐	
Fire Safety	Ignition sources	☐	
	Combustible Materials	☐	
	Hot Work (e.g. welding, grinding)	☐	
Other hazards	Ionizing radiation	☒	Measurements will be performed with 111mCd, therefore a zone properly classified should be available for the equipment during the experiments.